Journal of Applied Polymer Science

Facile fabrication of superhydrophobic polyimide/polytetrafluoroethylene composite coatings with high water adhesion

Yonggang Guo,[1] Zhongying Wang,[1] Haihong Wu,[1] Xia Zhang[2]

[1]School of Mechanical and Electrical Engineering, Henan University of Technology, Zhengzhou 450007, People's Republic of China

[2]Key Laboratory for Special Functional Materials of the Ministry of Education, Henan University, Kaifeng 475001, People's Republic of China

Correspondence to: Y. Guo (E-mail: nanogyg@163.com) and X. Zhang (E-mail: zhangxia2112@sohu.com)

ABSTRACT: A facile casting method was used to fabricate superhydrophobic polyimide/polytetrafluoroethylene composite coatings with high water adhesion. The water contact angles of the composite coatings were larger than 150°, expressing superhydrophobic property. But water droplets pinned tightly on the composite coating, even if it was upside down. The X-ray photoelectron spectrum analysis indicated that polyimide and polytetrafluoroethylene coexisted in the resulting coating. The observation with scanning electron microscopy showed that the composite coating formed lotus-like structure with many spherical polyimide papillae randomly bonding on the surface. But the tops of the polyimide papillae were not covered by lance-shaped Teflon fibres, forming an inhomogenous and discontinuous surface structure. This special surface chemical distribution and lotus-like structure combined to contribute to the high adhesive superhydrophobicity. This simple method may greatly extend the application range of high adhesive superhydrophobic surfaces in microcontrollable and microfluidic application. © 2015 Wiley Periodicals, Inc. J. Appl. Polym. Sci. **2015**, *132*, 42810.

KEYWORDS: coatings; composites; porous materials; surfaces and interfaces

Received 9 June 2015; accepted 4 August 2015

DOI: 10.1002/app.42810

INTRODUCTION

It is well known that combining hierarchical micro/nanostructures and low-surface-energy materials modification can achieve superhydrophobic surfaces with water contact angle (CA) larger than 150°.[1–3] Due to excellent self-cleaning effect, the ideal superhydrophobic surfaces with an extremely low sliding angle (SA) inspired by lotus leaf have attracted increasing attention for both fundamental research and practical applications.[4–8] However, some novel superhydrophobic surfaces in nature with high water adhesion, such as gecko feet, rose petals, scallions, and garlic,[9–12] have recently also attracted wide scientific interest because of their most outstanding application in no-loss microdroplet transportation known as a mechanical hand.[13–16] Especially, Jiang *et al.* demonstrated a "clinging-microdroplet" method to fabricate patterning crystal arrays based on the employment of high-adhesion, superhydrophobic surfaces,[17] which greatly extended the scope of application. In addition, the ability to position or fix tiny drops of liquid can be very valuable in providing platform for accurate biochemical analysis and smart microfluid devices.[18–20] Lots of effort has been done to mimic these high adhesive biological surfaces, although their fabrication is quite a challenge in searching a simple, time-saving, and easy-to-operate method.[21–24]

In this article, a facile and environmentally friendly one-step casting method was used to prepare polyimide/polytetrafluoroethylene composite coatings under a mild condition. The obtained composite coatings exhibit a micro/nanobinary structure and chemical heterogeneous composition. The CAs of the resulting composite coatings are larger than 150°, but water droplets can pin tightly on the surface even when the substrate is turned upside down, showing an excellent adhesive property. This facile preparation technology may provide a prospective future for the large-scale production and industrial application of adhesive superhydrophobic surfaces.

EXPERIMENTAL

Materials

Polyimide (PI) powders (Type YS-20) with particles size $<75\,\mu m$ and specific density of $1.4\,g/cm^3$ were provided by Shanghai Research Institute of Synthetic Resins (China).[25,26] Polytetrafluoroethylene (PTFE) concentrated dispersion (60 wt %)

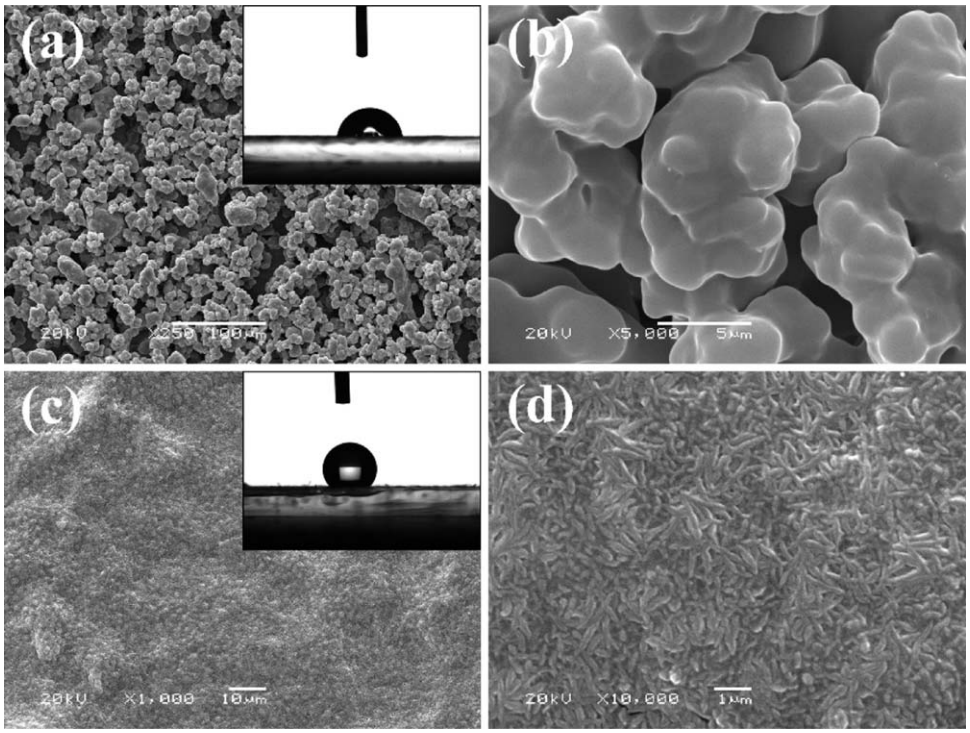

Figure 1. SEM images of pure PI (a, b) and pure PTFE (c, d) coatings, and the inset is the photograph of water droplet on the surface.

was purchased from Aladdin Industrial (Shanghai, China) and used as received. Anhydrous alcohol (Sinopharm Chemical Reagent) and glass slide (Nantong Hailun Bio-medical Apparatuses Manufacturing) are also used as received.

Preparation of PI/PTFE Composite Coatings

The PI/PTFE composite coating was prepared via a one-step casting process, which was carried out as follows. At first, 0.4 g PI was dispersed in 10 mL anhydrous alcohol by ultrasonic. Then PTFE concentrated dispersion was dispersed in the above solution with a mass ratio to PI of 1 : 2, 2 : 2, 3 : 2, 4 : 2, and 5 : 2 and stirred magnetically for 1 h. When the solution was homogenized by stirring, 100 μL of the mixture solution was cast on a clean glass slide and dried at ambient temperature (25 °C) for 20 min. Finally, the PI/PTFE composite coatings were obtained by curing the above drying coatings in an oven at 380 °C for 15 min. In addition, pure PI and PTFE coatings were prepared with the same method.

Characterization

Morphologies of the products were measured by scanning electron microscopy (SEM, JSM-5600 LV). The composition of the product was characterized by X-ray photoelectron spectrometer (XPS). The XPS was collected on an axis ultra X-ray photoelectron spectrometer, using mono-Al Kα X-ray as the excitation sources. Sessile water CA values were acquired using a DSA-100 optical CA meter (Kruss Company, Germany) at ambient temperature (25 °C). CAs were determined using the Laplace-Young fitting algorithm. Average CA values were obtained by measuring the sample at five different positions. Images were captured with a camera (Sony, Japan).

RESULTS AND DISCUSSION

Surface Morphology and Wettability of the Pure PI and Pure PTFE Coatings

Smooth PI film has a CA below 65 °,[27] indicating it is a kind of hydrophilic material. Pure PI coating was obtained when dropping the suspension of 0.4 g PI and 10 mL anhydrous alcohol on the glass slide, followed by drying at ambient temperature (25 °C) for about 20 min and curing in an oven at 380 °C for 15 min. The water CA of the resultant pure PI coating is about 88.4 ° [see the inset of Figure 1(a)]. Figure 1(a,b) show the SEM images of the pure PI coating with different magnifications. It is clear that the glass substrate is completely covered by many granular microspheres with diameter ranging from 5 to 8 μm. These microspheres are scattered here and there, forming porous network structure. The higher-magnification SEM image [Figure 1(b)] demonstrates these microspheres surface is very glossy and compact with few pores.

Similarly, dropping the diluent of 1.0 g PTFE concentrated dispersion with 10 mL anhydrous alcohol on the glass slide followed by drying at ambient temperature (25 °C) for about 20 min and curing in an oven at 380 °C for 15 min, we acquired the pure PTFE coating [as shown in Figure 1(c,d)]. At 380 °C the PTFE melted completely and kept in fusion state.[28,29] After cooling solidification, it can be seen from Figure 1(c) that the pure PTFE coating looks really flat, although the enlarged SEM image [Figure 1(d)] shows that there are many lance-shaped Teflon fibres on the coating surface. These fibres are very tiny and connect tightly to one another with small roughness. But because of the low surface energy of fluorine carbon structure this pure PTFE coating is hydrophobic with a static water CA of 136.4 ° as shown in the inset of Figure 1(c).

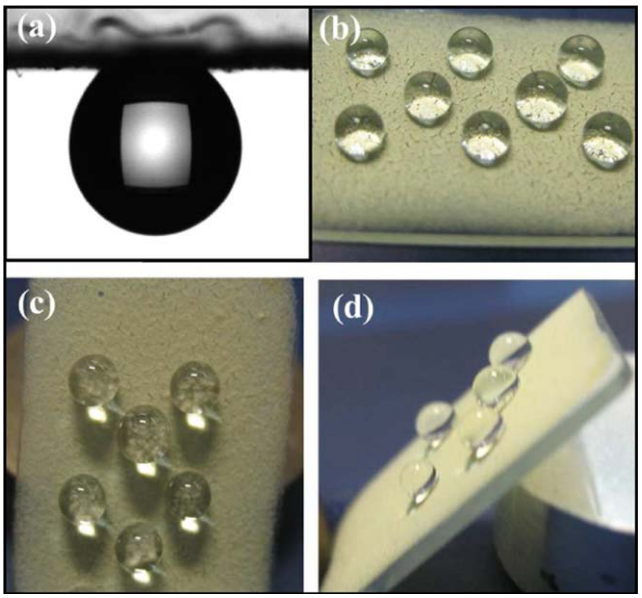

Figure 2. Photographic images showing some water droplets floating on PI/PTFE composite coatings with different tilt angles. (a) 180°, (b) 0°, (c) 60°, and (d) 45°. [Color figure can be viewed in the online issue, which is available at wileyonlinelibrary.com.]

Surface Wettability of the PI/PTFE Coatings

It can be seen from the above analysis that PI is hydrophilic material, while PTFE is hydrophobic. What is the wettability of the composite coating consisted of PI and PTFE? As shown in Figure 2(b), the PI/PTFE composite coating strongly repels the water with a CA larger than 150°. But what is interesting here is that, unlike water droplets freely rolling on the superhydrophobic lotus leaf, water drops pinned tightly on the PI/PTFE composite coating even it is tilted from 0° to 180° [Figure 2(a–d)], indicating a high adhesion between the coating and water droplets. In addition, after storage in air for 3 months, the CA value had almost no change, indicating that the superhydrophobicity was stable.

Surface Chemical Compositions of the Pure PI, Pure PTFE, and PI/PTFE Coatings

Figure 3 shows the XPS analysis results, which were carried out to determine the surface composition of the pure PI, pure PTFE and PI/PTFE composite coatings, respectively. The XPS results (Figure 3) clearly show that the elements such as F, O, N, and C are found in the PI/PTFE composite coating. The peak located at 399.4 eV is attributed to the N_{1s} of PI [Figure 3(a)], which is consistent with the accepted binding energy value for N_{1s} in PI.[30,31] But compared with the pure PTFE coating [Figure 3(b)], the peaks of F_{1s} and F_{KLL} appear in the XPS spectrum of the PI/PTFE composite coating [Figure 3(c)], indicating PI and PTFE coexist on the surface.

Surface Morphology of the PI/PTFE Coatings

Figure 4 is the SEM image of PI/PTFE composite coatings with different mass ratios at different magnifications. It can be seen from the low magnification images that many spherical papillae randomly bonding on the surface with diameter ranging from 5 to 15 μm. As shown in Figure 4, there are a few papillae distributed on the surfaces of the PI/PTFE composite coatings. Obviously, the microstructure of the composite coatings is different from the pure PI coating, on which plenty of microspheres-like PI has stacked up (as shown in Figure 1). When you look closely at higher-magnification SEM images [Figure 4(c,e,g,j)], you will see that the tops of the papillae are very smooth, while the rest of the papillae, from the middle to the bottom, are all covered with lance-shaped Teflon nanofibres. Obviously, the obtained surface exhibits a micro/nanobinary structure, consisting of microscale spherical papillae and nanoscale fibres. It is clear that the microstructure of the PI/PTFE composite coatings is very similar to that of the lotus leaf.[32] Compared with the SEM images of pure PI and pure PTFE coatings shown in Figure 1, we can easily find that the smooth tops of the papillae are made up of pure PI, whereas other parts below the top of papillae are completely covered by the lance-shaped PTFE fibres. That is to say, the PI papillae are not fully covered by continuous PTFE, leaving the tops of the papillae made up of hydrophilic PI.

In fact, the forming process of the PI/PTFE composite coating can be divided into three stages. At first, phase separation will occur to form PI agglomerations. The ethanol is a good dispersing agent for the PTFE concentrated dispersion. By contrast, the PI powders will precipitate and thus self-aggregate to form many papillae. In the meantime, PTFE with a better dispersion is still in the mixed solution of ethanol and PTFE aqueous dispersion. Then in the subsequent process of solvent evaporation, the PTFE concentrated dispersion will only cover on the middle and lower segments of the PI papillae. Finally in the PTFE melting and solidification stage, the molten PTFE still cannot cover the top of the papillae, forming a sharp contrast between the smooth PI top and lance-shaped PTFE underpart. This particular surface chemical composition distribution along with the lotus-like structure will undoubtedly have a significant effect on the wettability of the PI/PTFE composite coatings, namely the special high adhesive superhydrophobicity is attributed to the unique surface morphology and chemical composition.

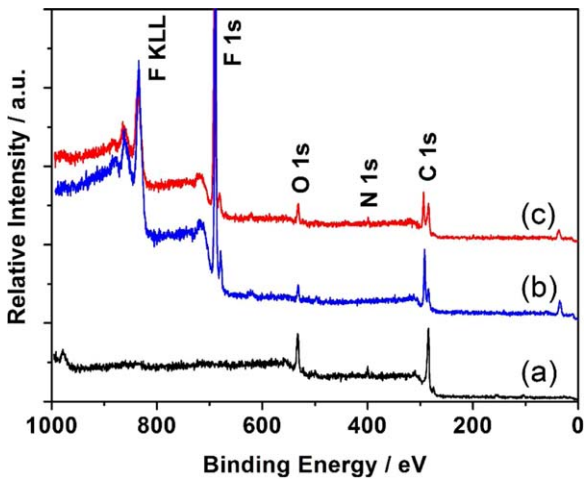

Figure 3. The XPS survey spectra of the pure PI (a), pure PTFE (b), and PI/PTFE (c) coatings. [Color figure can be viewed in the online issue, which is available at wileyonlinelibrary.com.]

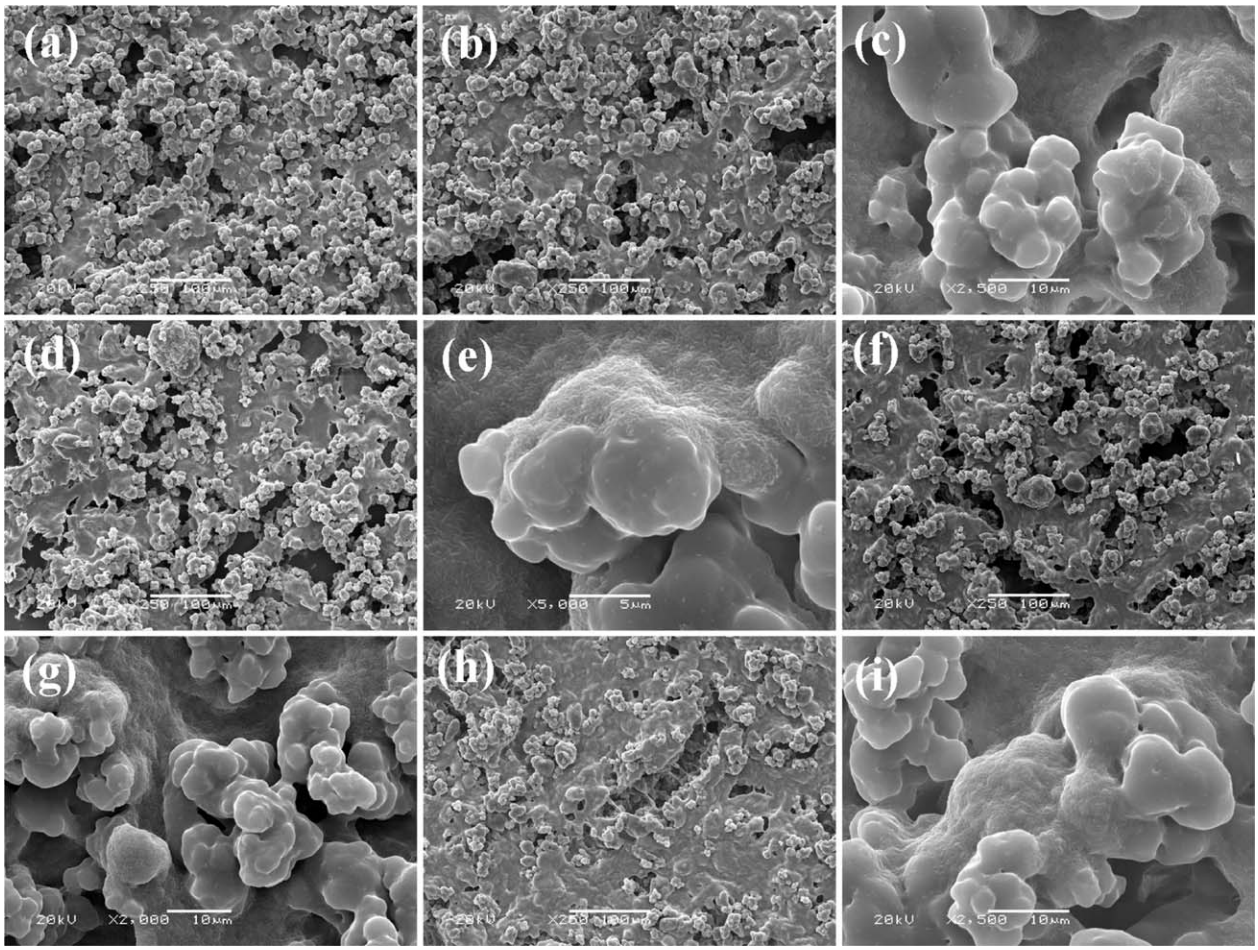

Figure 4. SEM images of PI/PTFE composite coatings with different mass ratios of PTFE to PI at different magnifications. (a) 1 : 2, (b, c) 2 : 2, (d, e) 3 : 2, (f, g) 4 : 2, and (h, i) 5 : 2.

The Effect of Mass Fraction of PTFE on the Wettability of the PI/PTFE Coatings

The wettability of PI/PTFE composite coatings was investigated with the mass fraction of PTFE increased while the mass of PI unchanged. It should be noted that if the amount of PTFE is smaller, especially when the mass ratio of PTFE to PI is lower than 1 : 2, the CA of the resulting PI/PTFE composite coating is lower than 150°. So we suppose in the study that the mass ratio of PTFE to PI is greater than 1 : 2. The variation of average water CAs and SAs at different mass ratios of PTFE to PI was shown in Figure 5. It could be seen that with the increase of the amount of PTFE, the CAs of the as-prepared PI/PTFE composite coatings increased slightly from 150.4° to 154.5°, indicating that the PTFE content had little or no significant effect on the CAs. The SAs of the composite coatings were always much greater than 45°, although the CAs kept larger than 150°. When the mass ratio of PTFE and PI was 1 : 2, the water droplet pinned on the composite coating even if the substrate was inverted. And then, as the mass of PTFE continued to increase, the SAs of the composite coatings first decreased from 58° to 45.1° then increased to 58.6°. The decrease of SA could be attributed to the increased PTFE, which was more hydrophobic, resulting in the lower adhesion between water droplets and the composite coating. On the other hand, as the mass fraction of PTFE further increased, the amount of spherical papillae reduced, which caused less air to be trapped

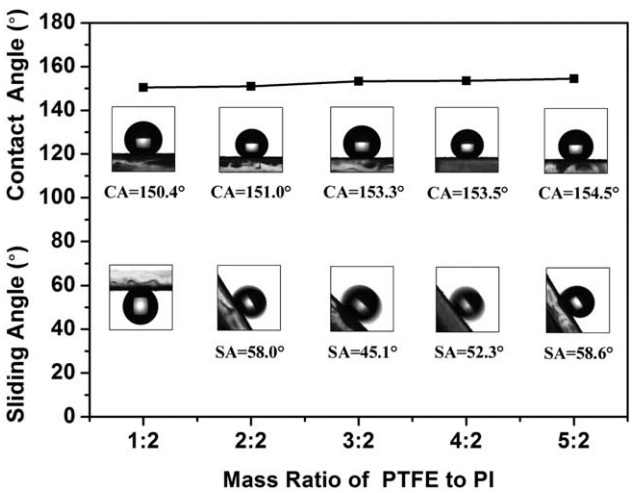

Figure 5. The variation of average water CA and SA at different mass ratios of PTFE to PI. The inset is the corresponding profile of a water droplet on the surface.

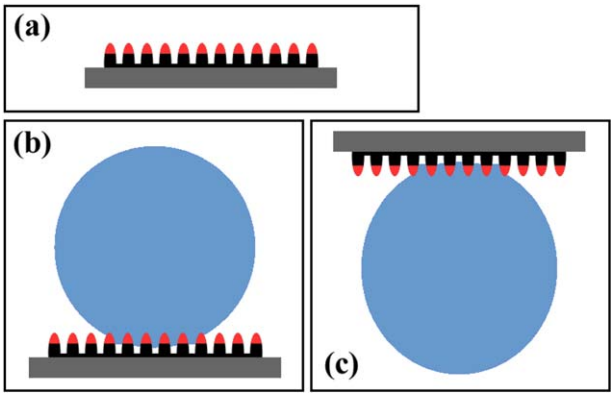

Figure 6. Schematic diagram of the as-prepared PI/PTFE composite coating (a) and the action model between the resulting surface and a water droplet (b, c). [Color figure can be viewed in the online issue, which is available at wileyonlinelibrary.com.]

between the coating and water droplets. Two major mechanisms assume that water exists presumably in Wenzel or Cassie state on hydrophobic surfaces.[33,34] For the Wenzel state, water droplets meet the solid surface, inducing a pinning state. For the Cassie state, water partially contacts with the solid due to the existence of air trapped at the rough surface, which makes water droplets easily rolling similar to the lotus leaf.[35] It is obvious that decreasing the amount of papillae to trap less air will help to transform the rolling Cassie state to the pinning Wenzel state, which can explain the slight decline of the SA.

Schematic Diagram of the Resulting High Adhesive Superhydrophobicity

In fact, the complex surface morphology of the PI/PTFE composite coating can be simplified to the schematic diagram as shown in Figure 6(a), in which the topmost of the PI papillae, marking in red, are hydrophilic PI, while both the lower part of the PI papillae and the junctions on the bottom of papillae, marking in black, are full fluorinated by PTFE. Since water is a polar molecule, it is easy to generate a strong interaction resulting from the strong hydrogen bonding between the water molecules and the hydrophilic groups. Because PTFE is a hydrophobic material, however there is a less interaction between water and the fluorinated regions even if van der Waals force exists. As Figure 6(b) displays, on the surface of porous PI/PTFE composite coating, both the air wrapped in the cavities and the PTFE hydrophobic regions strongly repel water droplet, resulting in the static water CA greater than 150°. On the other hand, the hydrophilic regions, although only exist on the tops of PI papillae which look very smooth as shown in Figure 4, can attract water droplet through the formation of hydrogen bonding between water molecules and carbonyl groups of the PI macrochains, which contributes to a macroscopically pinning state of a water drop on an inverted surface as shown in Figure 6(c).

The adhesion here produced by hydrophilic regions is totally different from those come from either water penetrating into the porous structure or van der Waals' force or Wenzel state or contact line pinning induced by hydrophobic defects.[10,12,24] Specially, some adhesive superhydrophobic surfaces induced by surface chemical compositions had to use expensive materials and complex process. For example, Zhou *et al.* attained adhesive superhydrophobicity through the anchor effect of surface grafted responsive polymer chains.[36] Using the amphiphilic polyurethane, Xu *et al.* considered that the interesting no-sliding superhydrophobic behavior is attributed to heterogeneous surface composition with both hydrophobic and hydrophilic domains on nanoscale.[37] Milionis *et al.* fabricated superhydrophobic surfaces with well-controlled water adhesion by spraying particles of different chemistries and sizes on a micropatterned surface. The theoretical and experimental data even proved that the wetting state of the sticky superhydrophobic surface they acquired conformed to the Cassie regime.[38] By contrast, the simple and effective casting method involved in this article does not need complicated equipment and expensive raw materials, which can help speed up the widespread use of the superhydrophobic surfaces with high adhesion in microfluidics, smart coatings, and biochemical analysis.

CONCLUSION

In conclusion, we have reported a simple and industry compatible approach to prepare superhydrophobic composite coating with high water adhesion. The resultant PI/PTFE composite coating exhibits a lotus-like microstructure consisting of microscale spherical papillae and nanoscale PTFE fibres. More interestingly, the PI papillae are not fully fluorinated by PTFE fibres, leaving only the topmost of the PI papillae is hydrophilic PI. This kind of particular surface chemical composition distribution along with the lotus-like structure contributes to the high adhesive superhydrophobicity. As the increase of the amount of PTFE, the CAs of the PI/PTFE composite coatings increased slightly, but the SAs first decreased then increased. The decrease of SA is attributed to the increased PTFE, while the reason for the followed increase of SA is that reduced spherical papillae on the coating cause less air to be trapped between the coating and water droplet. This is an easy, environmentally friendly and economical method for making adhesive superhydrophobic coatings, which can to a great extent bring more many advantages in the potential applications.

This work was supported by the Joint Talent Cultivation Funds of NSFC-Henan (U1404516, U1304529), National Natural Science Foundation of China (21403055, 51373048), Fundamental Research Funds for the Henan Provincial Colleges and Universities in Henan University of Technology (2014YWQQ06), Plan For Scientific Innovation Talent of Henan University of Technology (2013CXRC04), High Level Talents Foundation of Henan University of Technology (2011BS048), Henan Province Science and Technology Research Projects (142102210413), Natural Science Foundation of Henan Educational Committee (14B430001) and State Scholarship Fund of China.

REFERENCES

1. Bhushan, B.; Jung, Y. C. *Prog. Mater. Sci.* **2011**, *56*, 1.
2. Ju, J.; Wang, T.; Wang, Q. *J. Appl. Polym. Sci.* **2015**, *132*, 42077.

3. Zhang, X.; Guo, Y.; Zhang, P.; Zhang, Z.; Wu, Z. *ACS Appl. Mater. Interface* **2012**, *4*, 1742.
4. Lin, J.; Zheng, C.; Ye, W. J.; Wang, H. Q.; Feng, D. Y.; Li, Q. Y.; Huan, B. W. *J. Appl. Polym. Sci.* **2014**, *132*, 41458.
5. Zhang, X; Guo, Y; Zhang, Z.; Zhang, P. *Appl. Surf. Sci.* **2013**, *284*, 319.
6. Rianasari, I.; Weston, J.; Rowshan, R.; Blanton, T.; Khapli, S.; Jagannathan, R. *J. Appl. Polym. Sci.* **2015**, *132*, 41360.
7. Zhang, X.; Guo, Y.; Chen, H.; Zhu, W.; Zhang, P. *J. Mater. Chem. A* **2014**, *2*, 9002.
8. Li, F.; Du, M.; Zheng, Q. *J. Appl. Polym. Sci.* **2015**, *132*, 41500.
9. Feng, L.; Zhang, Y.; Xi, J.; Zhu, Y.; Wang, N.; Xia, F.; Jiang, L. *Langmuir* **2008**, *24*, 4114.
10. Chang, F. M.; Hong, S. J.; Sheng, Y. J.; Tsao, H. K. *Appl. Phys. Lett.* **2009**, *95*, 064102.
11. Autumn, K.; Liang, Y. A.; Hsieh, S. T.; Zesch, W.; Chan, W. P.; Kenny, T. W.; Fearing, R.; Full, R. J. *Nature* **2000**, *405*, 681.
12. Bhushan, B.; Her, E. K. *Langmuir* **2010**, *26*, 8207.
13. Hong, X.; Gao, X.; Jiang, L. *J. Am. Chem. Soc.* **2007**, *129*, 1478.
14. Wang, C. F.; Hsueh, T. W. *J. Phys. Chem. C* **2014**, *118*, 12399.
15. Li, J.; Jing, Z.; Zha, F.; Yang, Y.; Wang, Q.; Lei, Z. *ACS Appl. Mater. Interfaces* **2014**, *6*, 8868.
16. Long, J.; Fan, P.; Gong, D.; Jiang, D.; Zhang, H.; Li, L.; Zhong, M. *ACS Appl. Mater. Interfaces* **2015**, *7*, 9858.
17. Su, B.; Wang, S.; Ma, J.; Song, Y.; Jiang, L. *Adv. Funct. Mater.* **2011**, *21*, 3297.
18. Orner, B.; Derda, R.; Lewis, R. L.; Thomson, J. A.; Kiessling, L. L. *J. Am. Chem. Soc.* **2004**, *126*, 10808.
19. Rane, T. D.; Puleo, C. M.; Liu, K. J.; Zhang, Y.; Lee, A. P.; Wang, T. H. *Lab Chip* **2010**, *10*, 161.
20. Yu, Q.; Zeng, Z.; Zhao, W.; Li, M.; Wu, X.; Xue, Q. *Colloids Surf. A* **2013**, *427*, 1.
21. Cheng, Z. J.; Feng, L.; Jiang, L. *Adv. Funct. Mater.* **2008**, *18*, 3219.
22. Zhao, X. D.; Fan, H. M.; Luo, J.; Ding, J.; Liu, X. Y.; Zou, B. S.; Feng, Y. P. *Adv. Funct. Mater.* **2011**, *21*, 184.
23. Li, C.; Guo, R. W.; Jiang, L. *Adv. Mater.* **2009**, *21*, 4254.
24. Jin, M.; Feng, X.; Feng, L.; Sun, T.; Zhai, J.; Li, T.; Jiang, L. *Adv. Mater.* **2005**, *17*, 1977.
25. Zhao, G.; Hussainova, I.; Antonov, M.; Wang, Q.; Wang, T. *Wear* **2013**, *301*, 122.
26. Bao, L.; Lv, K.; He, F.; Qiu, Z. Chinese Pat. CN102108124A, June 29, **2011**.
27. Bellel, A.; Sahli, S.; Raynaud, P.; Segui, Y.; Ziari, Z.; Eschaich, D.; Dennler, G. *Plasma Process. Polym.* **2005**, *2*, 586.
28. Jiang, C.; Hou, W.; Wang, Q.; Wang, T. *Appl. Surf. Sci.* **2011**, *257*, 4821.
29. Hou, W.; Wang, Q. *J. Colloid Interfaces Sci.* **2009**, *333*, 400.
30. Han, M. G.; Im, S. S. *Polymer* **2000**, *41*, 3253.
31. Lee, K. W.; Gaynes, M. A.; Duchesne, E. *Electron. Mater. Lett.* **2006**, *2*, 171.
32. Neinhuis, C.; Barthlott, W. *Ann. Bot.-London* **1997**, *79*, 667.
33. Wenzel, R. N. *Ind. Eng. Chem.* **1936**, *28*, 988.
34. Cassie, A. B. D.; Baxter, S. *Trans. Faraday Soc.* **1944**, *40*, 546.
35. Dong, T.; Zhou, Y.; Hu, D.; Xiao, P.; Wang, Q.; Wang, J.; Pei, J.; Cao, Y. *J. Colloid Interface Sci.* **2015**, *445*, 213
36. Liu, X.; Ye, Q.; Song, X.; Zhu, Y.; Cao, X.; Liang, Y.; Zhou, F. *Soft Matter* **2011**, *7*, 515.
37. Zhao, N.; Xie, Q.; Kuang, X.; Wang, S.; Li, Y.; Lu, X.; Tan, S.; Shen, J.; Zhang, X.; Zhang, Y.; Xu, J.; Han, C. C. *Adv. Funct. Mater.* **2007**, *17*, 2739.
38. Milionis, A.; Martiradonna, L.; Anyfantis, G. C.; Cozzoli, P. D.; Bayer, I. S.; Fragouli, D.; Athanassiou, A. *Colloid Polym. Sci.* **2013**, *291*, 401.